

Numerical Runge- Kutta (4, 4) Method to Determine the Initial Configurations of the Jupitar Proto Planet Formed Via Disk Instability

M. S. Ali^{a*}, M. A. A. Mamun^b, M. M. Rahman^c, R. R. Mondal^d

^aAssistant Professor, Department of Mathematics, Bangabandhu Sheikh Mujibur Rahman Science and Technology University, Gopalganj-8100, Dhaka, Bangladesh

^{b,c}Lecturer of Mathematics, Bangladesh Army University of Engineering & Technology (BAUET), Natore-6431, Bangladesh

^dResearch student, Department of Mathematics, Bangabandhu Sheikh Mujibur Rahman Science and Technology University, Gopalganj-8100, Dhaka, Bangladesh

^aEmail: sali4222@gmail.com

^bEmail: masudarmath@gmail.com

Abstract

Numerical computational technique(s) with simulation tool is one of the most important difficult tasks in order to carry out real time scientific astronomical and other sophisticated problems. The main focus and highlight of this paper is concerned with the introduction of a method Runge-Kutta (4, 4) technique to determine the distribution of thermodynamic variables inside protoplanets during pre-collapse stage, formed by gravitational instability, for protoplanetary masses between 0.3 to 10 Jupiter. The case of convection is a significant concern for transference of heat inside the protoplanets and the graphical solution demonstrates positively better performance by the RK (4, 4) algorithm for any length of time. A viable quantitative analysis has been carried out to clearly visualize the goodness and robustness of the Runge-Kutta (4, 4) algorithm.

Keywords: Runge- Kutta (4, 4) Algorithm; Jupitar Protoplanet; Schwarzschild transformations; Clapeyron Equation; Disk Instability Models.

* Corresponding author.

1. Introduction

The mechanism of giant planet formation is one of the eminent topics of interest to scientists and still is a matter of debate. The discovery of the first extra solar planet in the mass range~0.5–3 Jupiter masses demands a reevaluation of theoretical mechanisms for giant planet formation (Boss [1]) and after that a lot of work has been done on the physical conditions prevailing in the interior of such planets both inside and outside the solar system (e.g., Helled and Schubert [2]; Boley and his colleagues [3]). Two mechanisms, available in the literature, i.e. the core accretion and disk instability models are the two end members that are used to explain the formation of gas giant planets.

According to the core accretion model, a heavy element core is formed first by the accretion of planetesimals. As the core becomes more massive, its gas accretion ability from the surrounding disk increases. When the core becomes sufficiently massive, rapid accretion of gas occurs onto the core, and a gas giant is formed (Pollack and his colleagues [4]; Hubickyj and his colleagues [5]; Matsuo and his colleagues [6]). With the difficulties encountered with the core accretion models, The only serious alternative of the currently favored core accretion model, the disk instability model, for explaining the formation of gaseous giant planets suggests that these planets are formed as a result of gravitational fragmentation in a massive protoplanetary disk surrounding a young star, the gravitational collapse of an unsegregated protoplanet which was in vogue in the 1970s when a great deal of now forgotten work has been reviewed and reformulated with fragmentation from massive protoplanetary disks, gas giants are formed due to local gravitational instability in the solar nebula having solar composition of elements and no core at all. This theory, once in vogue and then quickly forgotten, has been revived and reformulated by several authors (e.g. Boss [7]; Durisen, R. H and his colleagues [8], Cha and Nayakshin [9]; Boley and his colleagues [3]). As for example, the investigation of Nayakshin [10] predicted colder protoplanets than the ones found in Helled and Schubert [2] and Mayer and his colleagues [8] predicted denser and hotter protoplanets than the ones predicted by Boss [7].

However, no author has shown that such protoplanets with definite structure exists in reality. Boss [7] in his simulation assumed an initial protoplanet to be fully radiative, Helled and Schubert [2] found such protoplanets to be fully convective with a thin outer radiative zone, while Paul and his colleagues [11] and Senthilkumar and Paul [12] investigated the initial configurations of protoplanets assuming them to be fully convective. In this paper, we intend to investigate the internal structure of protoplanets formed by disk instability, using the distribution of necessary thermodynamic variables inside the gaint protoplanets obtained by solving their structure equations assuming the protoplanets to be fully convective.

1.1. Method Analysis

New innovative technique(s) continues to play a major role in research and development to obtain optimal solution (s) for any real-time problem(s). A large volume of work on initial value problems arising in Mathematics, engineering and physical sciences are being solved by the classic Runge-Kutta method. Evans and Yaakub [13] and Yaakub and Evans [14] introduced a new 4th order Runge–Kutta technique for initial value problems with error control. Evans and Yaakub [13] introduced a new fourth order Runge–Kutta method based

on the Heronian Mean formula for solving initial value problem in numerical analysis. In this article, the structure of initial extrasolar giant protoplanets having masses between 0.3 and 10 Jovian masses assuming the gas blob of the protoplanets to be fully convective have been analyzed and examined by RK (4,4) algorithm and the obtained results are addressed in detail.

1.2. Structure of the Protoplanets

For the initial grain radius we consider three different values, namely $r_0 = 10^{-1}$ cm, $r_0 = 10^{-2}$ cm and $r_0 = 10^{-3}$ cm. the object being formed via disk instability. Following Paul and his colleagues [11], such an object is assumed to be spherical with solar composition of gas, which is in a steady state of quasi-static equilibrium with no core in which the ideal gas law holds well.

In this paper, a giant gaseous protoplanet is referred to an object in the mass range 0.3Mj to 10Mj ($1Mj = 2 \times 1030$ g) and radius $R = 3 \times 10^{12}$ cm (Paul and his colleagues [11]) respectively.

1.3. Statement of the equations

This model assumes a non-rotating, non-magnetic spherical giant gaseous object of solar composition in the mass range 0.3–10 Jupiter masses. The choice of the mass range is that it covers most of the observed mass range of extra solar giant planets (see, e.g., Helled and Schubert [2]). As in DeCampi and Cameron [15] and Bodenheimer and his colleagues [16], in our study it is assumed that such an object is in a steady state of quasi-static equilibrium in which the ideal gas law holds and the gravitational contraction of the gas is only the source of energy. For heat transfer inside the object, we consider the convective case. Then the structure of the object during its pre-collapse stage can be given by the following set of equations:

The equation of hydrostatic equilibrium

$$\frac{dp(r)}{dr} = -\frac{GM(r)}{r^2} \rho(r)$$

The equation of conservation of mass,

$$\frac{dM(r)}{dr} = 4\pi r^2 \rho(r)$$

The equation of conservation heat flux

$$\frac{dT(r)}{dr} = -\left(1 - \frac{1}{\gamma}\right) \frac{T(r)}{p(r)} \frac{dP(r)}{dr}$$

The Clapeyron gas law,

$$P(r) = \frac{k}{\mu H} \rho(r)T(r)$$

In the above equations $P(r), T(r)$ and $\rho(r)$ represent the pressure, temperature and density respectively at distance r from the Centre of the protoplanet inside a radius r .

1.4. Essential boundary conditions

Let us consider a sphere of infinitesimal radius r at the Centre, We find that the mass of a protoplanet $M(r)$ is

$$M(r) = \frac{4}{3} \pi r^3 \rho(r)$$

Here ρ is the density. We may treat ρ sensibly constant in the sphere. Hence as $r \rightarrow 0$, it is also clear from the above equation that $M(r) = M$ at the surface.

We may derive suitable conditions for pressure and temperature of a protoplanet at its surface. The initial protoplanets having cold origin must have low surface temperature. In the first approximation we assume that the surface temperature is zero. So the approximate boundary conditions are

$$\left. \begin{aligned} T(r) = 0, P(r) = 0; & \text{ at } r = 0(\text{surface}) \\ M(r) = M; & \text{ at } r = R \\ M(r) = 0; & \text{ at } r = 0(\text{centre}) \end{aligned} \right\}$$

1.5. Solution of the equations

As is usual in numerical work, the equations were non-dimensionalized using the Schwarzschild transformations

$$P(r) = \frac{GM^2}{4\pi r^4} P, T(r) = \frac{\rho HGM}{KR} t, M(r) = qM, \text{ And } r = xR$$

With the help of above transformations and then using the transformation $x=1-y$

Then the following equations are given below.

The equation of the hydrostatic equilibrium

$$\frac{dP(r)}{dr} = - \frac{GM(r)\rho(r)}{r^2} \dots\dots\dots(1)$$

The equation of the conservation of mass

$$\frac{dM(r)}{dr} = 4\pi r^2 \rho(r) \dots\dots\dots(2)$$

The equation of convective heat flux

$$\frac{dT(r)}{dr} = \left(1 - \frac{1}{\gamma}\right) \frac{T(r)}{p(r)} \frac{dP}{dr} \dots\dots\dots(3)$$

The Clapeyron gas law

$$P(r) = \frac{K}{\mu H} \rho(r) T(r) \dots\dots\dots(4)$$

$$\text{and } M(r) = \frac{4}{3} \pi r^3 \rho(r) \dots\dots\dots(5)$$

We know $PV = RT$ and $\rho V = \text{mass of one gram molecule} = \mu \text{ gm}$, using Boltzmann Constant $K = RH$ we get

$$P = \frac{K}{\mu H} \rho T$$

Using the Schwarzschild transformation

$$P(r) = \frac{GM^2}{4\pi r^4} P, \quad T(r) = \frac{\rho HGM}{KR} t, \quad M(r) = qM, \quad \text{And } r = xR, \quad x = 1 - y$$

and boundary conditions

$$\left. \begin{aligned} T(r) = 0, P(r) = 0; \text{ at } r = 0(\text{surface}) \\ M(r) = M; \quad \text{at } r = R \\ M(r) = 0; \quad \text{at } r = 0(\text{centre}) \end{aligned} \right\} \dots\dots\dots(6)$$

Finally, equations (1),(2) and (3) can be reduced to the following form

$$\frac{dp}{dy} = \frac{pq}{t(1-y)^2}, \dots\dots\dots(7)$$

$$\frac{dq}{dy} = -\frac{p(1-y)^2}{t}, \dots\dots\dots(8)$$

and

$$\frac{dt}{dy} = \frac{2}{5} \frac{q}{(1-y)^2} \dots\dots\dots (9)$$

respectively where the value of γ is considered as $5/3$ is appropriate for a mono atomic gas.

While the boundary conditions given by equation (6) are reduced to the form

$$\left. \begin{array}{l} t=0, p=0, \quad \text{at } y=0 \\ q=1, \quad \quad \text{at } y=0 \\ q=1, \quad \quad \text{at } y=1 \end{array} \right\} \dots\dots\dots (10)$$

Solving equations (7) and (8) by using integration, we get

$$\therefore p = Et^{5/2} \dots\dots\dots (11)$$

Where E is a constant of integration.

Equation (4) can be reduces in the following form

$$\rho = \frac{M}{4\pi R^3} \frac{p}{t} \dots\dots\dots (12)$$

Also, differentiating both sides of equations (9) with respect to y and using equations (8) and (11), we get

$$\therefore \frac{1}{(1-y)^2} \frac{d}{dy} \left\{ (1-y)^2 \frac{dt}{dy} \right\} = \left(\frac{E}{2.5} \right) t^{1.5} \dots\dots\dots (13)$$

It is evident that if the equation (13) can be solved for t and $\frac{dt}{dy}$, then using equations (9) and (11), q and p can

be determined and hence using equation (12), ρ can be obtained. Equation (13) as such cannot be integrated analytically. Therefore, we must rely on numerical methods. However, integration cannot be started right from the surface. This complication arises from the fact that at the boundary vanishing denominators occur in the basic differential equations given by equation (13). Therefore, we have developed the solution at the boundary and have used the development to compute the solution at a point little distance from the boundary, and started step-by step integration procedure from this point. The forms of the variables used to integrate equation (13) are

$$t = \frac{2}{5} \frac{y}{(1-y)} \quad \text{and} \quad \frac{dt}{dy} = \frac{2}{5} \frac{1}{(1-y)^2} \quad \text{as } y \rightarrow 0. \quad \text{With these values as our initial conditions, we have solved}$$

equation (13) numerically by RK (4, 4) method to determine t and $\frac{dt}{dy}$ for different y . Following Paul and his colleagues [11] the value of E is supplied and through calibration, the value of E is adjusted. The correct value of E will be that for which the extra boundary condition $q \rightarrow 0$ as $y \rightarrow 1$ is satisfied. The value of E , through calibration, is found to be $E = 45.4$. In our numerical computation, the used values of mass and radius are those that are available in Helled and Schubert [2]. Also, we have used $\mu=2.2$, as is appropriate for molecular hydrogen, and all other values involved in the problem have been assumed to have their standard values.

1.6. Simulation results and analysis

The above figure shows that the distribution of thermodynamic variables central temperature and pressure inside the protoplanets with increasing Jupiter mass. The different color dotted line shows that the initial configuration for objects with Jupiter masses 0.3, 1, 5, 7 and 10 respectively. Figure 1 shows the pressure for 1.0 Jupiter mass and Figure 2 shows our calculated pressure profiles inside the protoplanets with the assumed masses. It can be shown from the figure that after a point little depth from the surface down to the core region, the pressures of the protoplanets at a corresponding point increase with their increasing masses, Figure 3 shows the temperature for 1.0 Jupiter mass. It can be shown from the figure 4 that the more massive is a protoplanet the hotter is its interior and for objects with Jupiter masses 0.3, 1, 5, 7 and 10 respectively it is very difficult to compare the profiles with each other. Figure 5 shows the density for 1.0 Jupiter mass and Figure 6 depicts the distribution of density inside the protoplanets assumed. It can be observed from the figure that the surface density of the protoplanets with masses 0.3, and 1 Jupiter masses decreases with decreasing masses. On the other hand the protoplanet with mass 10 Jupiter mass can be found to be rarer in comparison with the protoplanets with masses 5 and 7 Jupiter masses with respect to surface densities. Figure 4 shows our calculated pressure and temperature profiles inside the protoplanets with the assumed masses.

For increasing pressure of different masses the temperature is also increased. Figure 7 shows our calculated pressure and density profiles inside the protoplanets with the assumed masses. For increasing pressure of different masses the density is also increased. Figure 8 shows our calculated temperature and density profiles inside the protoplanets with the assumed masses. For increasing temperature of different masses the density is also increased but the density of 7 Jupiter mass is higher than the 10 Jupiter mass.

2. Conclusion

The Runge-Kutta (4, 4) method is analyzed mathematically and properly implemented in determining the distribution of thermodynamic variables inside protoplanets during pre-collapse stage, formed by gravitational instability for protoplanetary masses between 0.3 to 10 Jupiter masses. When the mass is larger than 0.3 Jupiter mass the central temperature of the protoplanets increased. As a result, the interior part (Convective) of the protoplanet is hotter with increasing Jupiter mass. This also shows that after a point little depth from the surface down to the core region, the pressures of the protoplanets at a corresponding point increase with their increasing masses. The all figures show that matter is not distributed uniformly in the atmosphere, and there may be variation in parameters due to gravitational stratification.

3. Limitations

It is important to mention here that Clapeyron equation of state is valid for gas at not very high pressure and temperature. The central pressure of the protoplanets in this case can be found to be the below 2×10^{-2} atm (Paul and his colleagues [11]). But this Clapeyron equation of state is not suitable at very low temperature and high pressure. Also, the gas is found to be not idealized, rather a composition of both ionized and non-ionized. Thus in this communication, we intend to investigate initial configuration of protoplanets formed via disk instability with the appropriate equation of state and to see how our computed results compare the results obtained in different investigation

3.1. Tables

Table 1: Mathematical results of pressure, temperature and density for 1.0 Jupiter mass

X	Pressure	Temperature	Density
0.0100000000000000	0.000000019176690	0.002525252525253	0.000000000000008
0.0200000000000000	0.001604924395652	20.187710437383400	0.000000000000081
0.0300000000000000	0.003268220129475	26.861784509080700	0.000000000000123
0.0400000000000000	0.004378360795089	30.196062659939000	0.000000000000147
0.0500000000000000	0.005139799402255	32.196268413705300	0.000000000000162
0.0600000000000000	0.005688591513147	33.529662954926200	0.000000000000172
0.0700000000000000	0.006101194398254	34.482066256753000	0.000000000000180
0.0800000000000000	0.006422084925875	35.196361403159100	0.000000000000185
0.0900000000000000	0.006678517654371	35.751921389557600	0.000000000000190
0.1000000000000000	0.006888015204260	36.196368091970900	0.000000000000193
0.1100000000000000	0.007062317552027	36.560005680092500	0.000000000000196
0.1200000000000000	0.007209570202987	36.863036678595600	0.000000000000198
0.1300000000000000	0.007335595199022	37.119447342565200	0.000000000000201
0.1400000000000000	0.007444661131065	37.339227804731400	0.000000000000202
0.1500000000000000	0.007539967174237	37.529704138312800	0.000000000000204
0.1600000000000000	0.007623957340847	37.696370885817200	0.000000000000205
0.1700000000000000	0.007698530368740	37.843429749536600	0.000000000000206
0.1800000000000000	0.007765183452545	37.974148716393400	0.000000000000208
0.1900000000000000	0.007825112876806	38.091107773885100	0.000000000000208
0.2000000000000000	0.007879285881003	38.196370910704000	0.000000000000209
0.2100000000000000	0.007928492898567	38.291608974034500	0.000000000000210
0.2200000000000000	0.007973386141455	38.378189020155600	0.000000000000211
0.2300000000000000	0.008014508514906	38.457240356099900	0.000000000000211
0.2400000000000000	0.008052315572966	38.529704070844600	0.000000000000212
0.2500000000000000	0.008087192391497	38.596370678985200	0.000000000000213
0.2600000000000000	0.008119466679007	38.657909077387700	0.000000000000213
0.2700000000000000	0.008149419068060	38.714889067017000	0.000000000000214
0.2800000000000000	0.008177291269574	38.767799048652000	0.000000000000214

0.2900000000000000	0.008203292590088	38.817060057412000	0.000000000000214
0.3000000000000000	0.008227605182721	38.863036990375500	0.000000000000215
0.3100000000000000	0.008250388309721	38.906047661108800	0.000000000000215
0.3200000000000000	0.008271781826918	38.946370156468800	0.000000000000216
0.3300000000000000	0.008291909050823	38.984248855804600	0.000000000000216
0.3400000000000000	0.008310879132243	39.019899387946200	0.000000000000216
0.3500000000000000	0.008328789032718	39.053512738422900	0.000000000000216
0.3600000000000000	0.008345725179156	39.085258672145200	0.000000000000217
0.3700000000000000	0.008361764856180	39.115288601057000	0.000000000000217
0.3800000000000000	0.008376977383398	39.143737999000200	0.000000000000217
0.3900000000000000	0.008391425115395	39.170728445061600	0.000000000000217
0.4000000000000000	0.008405164294805	39.196369360417600	0.000000000000218
0.4100000000000000	0.008418245783036	39.220759491006700	0.000000000000218
0.4200000000000000	0.008430715688643	39.243988178391400	0.000000000000218
0.4300000000000000	0.008442615909677	39.266136453290100	0.000000000000218
0.4400000000000000	0.008453984603457	39.287277979991700	0.000000000000218
0.4500000000000000	0.008464856594821	39.307479874847900	0.000000000000219
0.4600000000000000	0.008475263732075	39.326803418005300	0.000000000000219
0.4700000000000000	0.008485235198280	39.345304674278500	0.000000000000219
0.4800000000000000	0.008494797784285	39.363035036414100	0.000000000000219
0.4900000000000000	0.008503976128872	39.380041701832000	0.000000000000219
0.5000000000000000	0.008512792930551	39.396368092158400	0.000000000000219
0.5100000000000000	0.008521269134832	39.412054223401700	0.000000000000219
0.5200000000000000	0.008529424100214	39.427137033415500	0.000000000000220
0.5300000000000000	0.008537275745678	39.441650672290900	0.000000000000220
0.5400000000000000	0.008544840682021	39.455626760482300	0.000000000000220
0.5500000000000000	0.008552134329085	39.469094618774800	0.000000000000220
0.5600000000000000	0.008559171020592	39.482081473611500	0.000000000000220
0.5700000000000000	0.008565964098107	39.494612640808100	0.000000000000220
0.5800000000000000	0.008572525995405	39.506711690261700	0.000000000000220
0.5900000000000000	0.008578868314387	39.518400593910200	0.000000000000220
0.6000000000000000	0.008585001893486	39.529699858895800	0.000000000000220
0.6100000000000000	0.008590936869454	39.540628647629800	0.000000000000220
0.6200000000000000	0.008596682733225	39.551204886239100	0.000000000000221
0.6300000000000000	0.008602248380540	39.561445362683700	0.000000000000221
0.6400000000000000	0.008607642157876	39.571365815676100	0.000000000000221
0.6500000000000000	0.008612871904191	39.580981015392400	0.000000000000221
0.6600000000000000	0.008617944988914	39.590304836846900	0.000000000000221
0.6700000000000000	0.008622868346583	39.599350326694500	0.000000000000221
0.6800000000000000	0.008627648508451	39.608129764140000	0.000000000000221
0.6900000000000000	0.008632291631379	39.616654716550000	0.000000000000221
0.7000000000000000	0.008636803524284	39.624936090299000	0.000000000000221

0.7100000000000000	0.008641189672374	39.632984177317700	0.000000000000221
0.7200000000000000	0.008645455259383	39.640808697762800	0.000000000000221
0.7300000000000000	0.008649605187998	39.648418839179800	0.000000000000221
0.7400000000000000	0.008653644098656	39.655823292490100	0.000000000000221
0.7500000000000000	0.008657576386840	39.663030285099200	0.000000000000222
0.7600000000000000	0.008661406219035	39.670047611391300	0.000000000000222
0.7700000000000000	0.008665137547443	39.676882660847600	0.000000000000222
0.7800000000000000	0.008668774123588	39.6835424444001400	0.000000000000222
0.7900000000000000	0.008672319510889	39.690033616422300	0.000000000000222
0.8000000000000000	0.00867577096304	39.696362500901600	0.000000000000222
0.8100000000000001	0.008679150101118	39.702535107993800	0.000000000000222
0.8200000000000001	0.008682441590953	39.708557155055700	0.000000000000222
0.8300000000000001	0.008685654485053	39.714434083908800	0.000000000000222
0.8400000000000001	0.008688791564919	39.720171077240200	0.000000000000222
0.8500000000000001	0.008691855482340	39.725773073845900	0.000000000000222
0.8600000000000001	0.008694848766863	39.731244782810500	0.000000000000222
0.8700000000000001	0.008697773832759	39.736590696708900	0.000000000000222
0.8800000000000001	0.008700632985513	39.741815103908000	0.000000000000222
0.8900000000000001	0.008703428427886	39.746922100039200	0.000000000000222
0.9000000000000001	0.008706162265570	39.751915598705900	0.000000000000222
0.9100000000000001	0.008708836512476	39.756799341484700	0.000000000000222
0.9200000000000001	0.008711453095682	39.761576907275300	0.000000000000222
0.9300000000000001	0.008714013860065	39.766251721045900	0.000000000000222
0.9400000000000001	0.008716520572631	39.770827062021700	0.000000000000222
0.9500000000000001	0.008718974926588	39.775306071355000	0.000000000000222
0.9600000000000001	0.008721378545152	39.779691759316900	0.000000000000222
0.9700000000000001	0.008723732985132	39.783987012043500	0.000000000000223
0.9800000000000001	0.008726039740286	39.788194597869500	0.000000000000223
0.9900000000000001	0.008728300244486	39.792317173277700	0.000000000000223

4. Figures

Graphical representation of equation of state

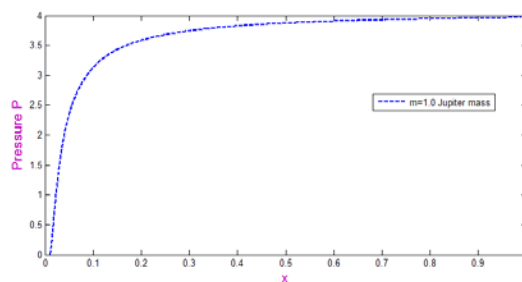


Figure 1: initial pressure profile of a protoplanet.

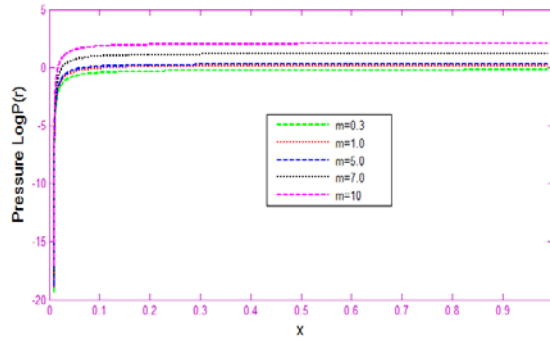


Figure 2: pressure profiles inside some initial protoplanets.

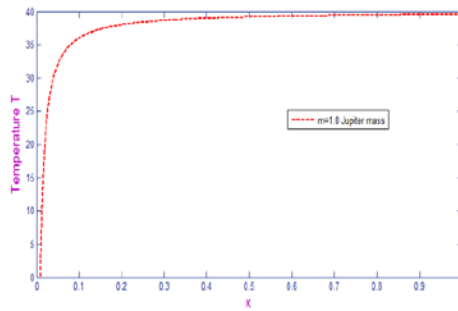


Figure 3: initial temperature profile of a protoplanet.

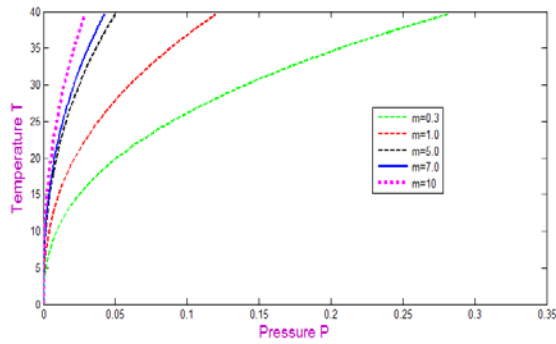


Figure 4: Pressure- Temperature profiles of some initial protoplanets.

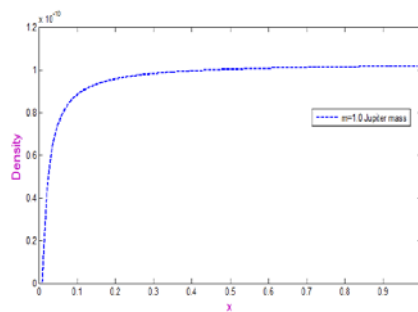


Figure 5: initial density profile of a protoplanet.

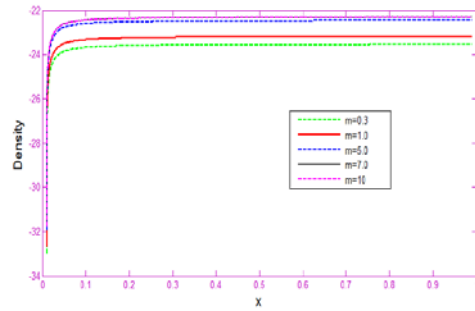


Figure 6: Density distributions of some initial protoplanets.

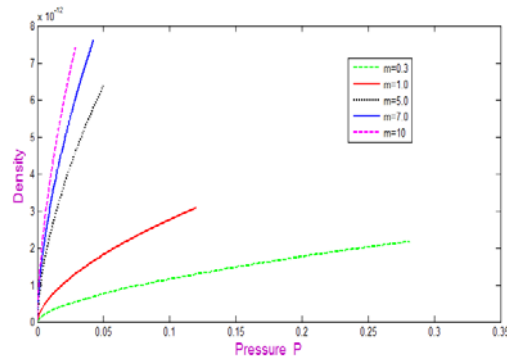


Figure 7: initial pressure-density profiles of some protoplanets.

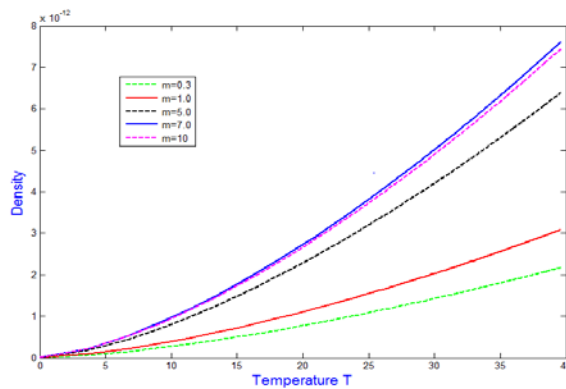


Figure 8: initial temperature-density profiles of some protoplanets.

References

- [1] Boss, A. P. "Formation of extrasolar giant planets: Core accretion or disk instability?." *Earth, Moon, and Planets* 81.1 (1998): 19-26.
- [2] Helled, Ravit, and Gerald Schubert. "Core formation in giant gaseous protoplanets." *Icarus* 198.1 (2008): 156-162.

- [3] Boley, Aaron C., et al. "Clumps in the outer disk by disk instability: Why they are initially gas giants and the legacy of disruption." *Icarus* 207.2 (2010): 509-516.
- [4] Pollack, James B., et al. "Formation of the giant planets by concurrent accretion of solids and gas." *icarus* 124.1 (1996): 62-85.
- [5] Hubickyj, Olenka, Peter Bodenheimer, and Jack J. Lissauer. "Accretion of the gaseous envelope of Jupiter around a 5–10 Earth-mass core." *Icarus* 179.2 (2005): 415-431.
- [6] Matsuo, Taro, et al. "Planetary formation scenarios revisited: Core-accretion versus disk instability." *The Astrophysical Journal* 662.2 (2007): 1282.
- [7] Boss, Alan P. "Testing disk instability models for giant planet formation." *The Astrophysical Journal Letters* 661.1 (2007): L73.
- [8] Durisen, R. H., et al. "Protostars and Planets V, ed." B. Reipurth, D. Jewitt, & K. Keil (Tucson: University of Arizona Press) p 607 (2007).
- [9] Cha, Seung-Hoon, and Sergei Nayakshin. "A numerical simulation of a 'Super-Earth' core delivery from ~ 100 to ~ 8 au." *Monthly Notices of the Royal Astronomical Society* 415.4 (2011): 3319-3334.
- [10] Nayakshin, Sergei. "Grain sedimentation inside giant planet embryos." *Monthly Notices of the Royal Astronomical Society* 408.4 (2010): 2381-2396.
- [11] Paul, G. C., J. N. Pramanik, and S. K. Bhattacharjee. "Gravitational settling time of solid grains in gaseous protoplanets." *Acta Astronautica* 76 (2012): 95-98.
- [12] Senthilkumar Sukumar, and Gour Chandra Paul. "Application of new RKAHeM (4, 4) technique to analyze the structure of initial extrasolar giant protoplanets." *Earth Science Informatics* 5.1 (2012): 23-31.
- [13] Evans, D. J., and A. R. Yaakub. "A new Runge Kutta RK (4, 4) method." *International journal of computer mathematics* 58.3-4 (1995): 169-187.
- [14] Yaakub, A. R., and David J. Evans. "A fourth order Runge–Kutta RK (4, 4) method with error control." *International journal of computer mathematics* 71.3 (1999): 383-411.
- [15] De Campli, William M., and A. G. W. Cameron. "Structure and evolution of isolated giant gaseous protoplanets." *Icarus* 38.3 (1979): 367-391.
- [16] Bodenheimer, Peter, Gregory Laughlin, and Douglas NC Lin. "On the radii of extrasolar giant planets." *The Astrophysical Journal* 592.1 (2003): 555.